

The Optical Gravitational Lensing Experiment Catalog of stellar proper motions in the OGLE-II Galactic bulge fields

T. Sumi¹, X. Wu¹, A. Udalski², M. Szymanski², M. Kubiak², G. Pietrzynski^{2,3},
I. Soszynski², P. Wozniak⁴, K. Zebun², O. Szewczyk² & L. Wyrzykowski²

¹ Princeton University Observatory, Princeton, NJ 08544-1001, USA; e-mail: (sumi, xiaoanwu)@astro.princeton.edu

² Warsaw University Observatory, Al. Ujazdowskie 4, 00-478 Warszawa, Poland;
e-mail: (udalski,mszm,kpietrzyn,soszynsk,zebrun,szewczyk,wyrzykow)@astrouw.edu.pl

³ Universidad de Concepcion, Departamento de Fisica, Casilla 160 (C, Concepcion, Chile

⁴ Los Alamos National Laboratory, MS-D 436, Los Alamos, NM 87545 USA; e-mail: wozniak@lanl.gov

Accepted Received in original form

ABSTRACT

We present proper motion (μ) catalog of 5,078,188 stars in 49 Optical Gravitational Lensing Experiment II (OGLE-II) Galactic bulge fields, with the total area close to 11 square degrees. The proper motion measurements are based on 138 555 I-band images taken during four observing seasons: 1997-2000. The catalogue stars are in the magnitude range $11 < I < 18$ mag. In particular, the catalogue includes Red Clump Giants (RCGs) and Red Giants in the Galactic Bulge, and main sequence stars in the Galactic disc. The proper motions up to $\mu = 500$ mas yr⁻¹ were measured with the mean accuracy of $0.8 - 3.5$ mas yr⁻¹, depending on the brightness of a star. This catalogue may be useful for studying the kinematics of stars in the Galactic Bulge and the Galactic disk.

Key words: Galaxy:bulge { Galaxy:center { Galaxy:kinematics and dynamics { Galaxy:structure { astrometry

1 INTRODUCTION

The Galactic Bulge is the nearest bulge in which individual stars can be studied in detail. A study of stellar populations and stellar dynamics in the Bulge may help us understand how bulges formed, what are their populations, gravitational potential and structure.

The proper motions with precise photometry might make it possible to separate the observed populations based on their kinematics. Such study has first been done by Spaenhauer, Jones & Whitford (1992) with photographic plates only for a few hundred of brightest red giants in Baade's window. Recently deeper study have been done by Kuijken & Rich (2002) with Hubble Space Telescope (HST)/WFC2 in Baade's window.

Several groups have carried out gravitational microlensing observations toward dense stellar fields, such as the Magellanic clouds, the Galactic center and disc. Until now, hundreds of events have been found (EROS: Aubourg et al. 1993; OGLE: Udalski et al. 2000; Wozniak et al. 2001; MACHO: Acock et al. 2000; MOA: Bond et al. 2001; Sumi et al. 2003), and thousands are expected in the up-

coming years by MOA¹, OGLE-III² and other collaborations.

It is well known that the gravitational microlensing survey data is well suited for numerous other scientific projects (see Paczynski 1996; Gould 1996). The studies of the Galactic structure certainly benefit from this type of data. The microlensing optical depth probes the mass density of compact objects along the line of sight and the event time-scale distribution is related to the mass function and kinematics of the lensing objects. Observed high optical depth may be explained by the presence of the bar (Udalski et al. 1994; Acock et al. 1997, 2000; Sumi et al. 2003; Afonso et al. 2003; Popowski et al. 2003). There is substantial evidence that the Galaxy has a bar at its center (de Vaucouleurs 1964; Blitz & Spergel 1991; Stanek et al. 1994, 1997; Kiraga & Paczynski 1994; Hafner et al. 2000). However, the parameters of the bar, e.g., its mass, size, and the motion of stars within it, still remain poorly constrained.

Stanek et al. (1997) used the Red Clump Giants (RCGs) to constrain the axial ratios and orientation of the

¹ <http://www.phys.canterbury.ac.nz/~physib/alert/alert.html>

² <http://www.astrouw.edu.pl/~ogle/ogle3/ews/ews.html>

arXiv:astro-ph/0305315v1 16 May 2003

Galactic bar. These stars are the equivalent of the horizontal branch stars for a metal-rich population, i.e., relatively low-mass core helium burning stars. RCGs in the Galactic bulge occupy a distinct region in the colour magnitude diagram (Stanek et al. 2000 and references therein). The intrinsic width of the luminosity distribution of RCGs in the Galactic bulge is small, about 0.2 mag (Stanek et al. 1997; Paczynski & Stanek 1998). Their observed peak and width of the luminosity function are related to the distance and radial depth of the bar.

Furthermore, Mao & Paczynski (2002) suggested that there should be a difference in average proper motions of 1.6 m asyr^{-1} between the bright and faint RCG sub-samples, which are on average on the near and the far side of the bar, respectively, if their tangential streaming motion is 100 km s^{-1} . Following this suggestion, Sumi, Eyer & Wozniak (2003) measured mean proper motion of bright and faint RCGs in one OGLE-II field in Baade's Window, and they found a difference to be $1.5 \pm 0.11 \text{ m asyr}^{-1}$.

To expand this analysis we measured proper motions in all 49 Galactic Bulge fields observed by the Optical Gravitational Experiment II (OGLE-II; Udalski et al. 2000) for stars down to $I = 18 \text{ mag}$, which is sufficiently deep to include RCGs. There are several earlier proper motion catalogues of this general area (c.f. USNO-B Monet et al. 2002, Improved NLTT Salim & Gould 2003 and Tycho-2 Høg et al. 2000). Though the area covered by our catalogue is relatively small, it reaches deeper and covers a wide range of proper motion ($< 500 \text{ m asyr}^{-1}$) with the accuracy as good as ($\sim 1 \text{ m asyr}^{-1}$). In §2 we describe the data. We present the analysis method in §3. Discussion and conclusion are given in §7.

2 DATA

We use the data collected during the second phase of the OGLE experiment, between 1997 and 2000. All observations were made with the 1.3-m Warsaw telescope located at the Las Campanas Observatory, Chile, which is operated by the Carnegie Institution of Washington. The "first generation" camera has a SITe 2048 \times 2048 pixel CCD detector with pixel size of $24 \mu\text{m}$ resulting in $0.417 \text{ arcsec/pixel}$ scale. Images of the Galactic bulge were taken in drift-scan mode at "medium" readout speed with the gain $7.1 \text{ e}^-/\text{ADU}$ and readout noise of 6.3 e^- . A single 2048 \times 8192 pixel frame covers an area of $0.24 \times 0.95 \text{ deg}^2$. Saturation level is about 55,000 ADU. Details of the instrumentation setup can be seen in Udalski, Kubiak & Szymanski (1997).

In this paper we use 138-555 I-band frames of the BUL_SC1-49 fields. Centre of these fields are listed in Table 1. The time baseline is almost 4 years. There are gaps between the observing seasons when the Galactic bulge cannot be observed from the Earth, each about 3 months long. The median seeing is $1.3''$. We use the VI photometric maps of standard OGLE template (Udalski et al. 2002) as the astrometric and photometric references.

Only about 70% of the area of the BUL_SC1 field overlaps with the extinction map made by Stanek (1996). The

extinction map covering all OGLE-II fields is in preparation, and it will be made public soon.

3 ANALYSIS

The analysis in this work follows Sumi, Eyer & Wozniak (2003), except our procedure makes it possible to detect high proper motions, and extends to the limiting magnitude down to $I = 18 \text{ mag}$. The standard OGLE template given by Udalski et al. (2002) serves as the standard astrometric reference in our analysis. In order to treat properly spatial PSF variations and frame distortions each OGLE-II field is divided into 256 subframes before processing. Subframes are 512×128 pixels with 14 pixel margin on each side to smooth out transitions between the local polynomials. The shape of the subframe reflects stronger y-axis (declination) distortions due to drift-scan mode of observation.

We compute the pixel positions of stars in each of the subframes using the DOPHOT package (Schechter, Mateo & Saha 1993). At the start of the processing for each exposure, the positions of stars in a single subframe are measured and cross-referenced with those in the template and the overall frame shift is obtained. Using this crude shift we can identify the same region of the sky (corresponding to a given subframe of the template) throughout the entire sequence of frames. For each subframe all stars with $I < 18 \text{ mag}$ (~ 400 of them, depending on the stellar density in each field) categorized by DOPHOT as isolated stars (marked as `type=1`) are used to derive the local transformation between pixel coordinate systems of a given exposure and the template. We don't use the data points categorized by DOPHOT as a star blended with other star (marked as `type=3`). The search radius in matching the stars between template and other frames is 1.0 pixel instead of 0.5 pix used in Sumi, Eyer & Wozniak (2003) to increase the range of detectable high proper motion objects. We estimate that the probability of the mis-identification in this search radius is negligible (0.26%).

We use a first order polynomial to fit the transformation. The resulting piece-wise transformation adequately converts pixel positions to the reference frame of the template. Typical residuals are at the level of 0.08 pixels for bright stars ($I < 16$) and 0.2 pixels for all stars ($I < 18$).

An example of time dependence of the position for a star with a moderate detectable proper motion is shown in Fig. 1 with filled circles. To measure the proper motion we fit the positions as a function of time with the following formula:

$$x = x_0 + \mu_x t + a \sin C \tan z; \quad (1)$$

$$y = y_0 + \mu_y t + a \cos C \tan z; \quad (2)$$

where a is the coefficient of differential refraction, z is the zenith angle, and C is the angle between the line joining the star and Zenith and the line joining the star with the South Pole, and x_0 and y_0 are constants. The parameter a is a function of the apparent star colour. We neglect the parallactic motion due to Earth's orbit because its effect is strongly degenerate with the effect of differential refraction for stars in the direction of the Galactic Bulge (Eyer & Wozniak (2001)).

³ see <http://www.astrouw.edu.pl/~ogle> or <http://bulge.princeton.edu/~ogle>

Table 1. Center positions of OGLE-II 49 fields. The number of frames N_f and stars N_s , and the mean of uncertainty in proper motion, $\langle \mu \rangle$ (mas yr^{-1}), are given as a function of I (mag) for each field. $\langle \mu \rangle$ is averaged over $I = 0.5$ mag.

eld	2000		l (deg.)	b (deg.)	N_f	N_s	$\langle \mu \rangle$ (mas yr^{-1}), for I (mag) =							
	RA	Dec					11.5	12.5	13.5	14.5	15.5	16.5	17.5	
BUL_SC 1	18 ^h 02 ^m 32.5 ^s	29 57 ^o 41 ⁰⁰	1.08	-3.62	259	120644	2.45	0.92	0.88	0.97	1.32	2.51	5.98	
BUL_SC 2	18 ^h 04 ^m 28.6 ^s	28 52 ^o 35 ⁰⁰	2.23	-3.46	264	140315	2.70	0.95	0.89	1.03	1.39	2.82	6.73	
BUL_SC 3	17 ^h 53 ^m 34.4 ^s	29 57 ^o 56 ⁰⁰	0.11	-1.93	555	167477	1.97	0.64	0.61	0.76	1.20	2.01	4.64	
BUL_SC 4	17 ^h 54 ^m 35.7 ^s	29 43 ^o 41 ⁰⁰	0.43	-2.01	514	179808	2.34	0.67	0.67	0.87	1.42	2.49	5.70	
BUL_SC 5	17 ^h 50 ^m 21.7 ^s	29 56 ^o 49 ⁰⁰	-0.23	-1.33	392	113747	2.01	0.77	0.72	0.82	1.10	2.02	3.53	
BUL_SC 6	18 ^h 08 ^m 03.7 ^s	32 07 ^o 48 ⁰⁰	-0.25	-5.70	306	65562	1.79	0.89	0.83	0.91	1.21	2.20	4.43	
BUL_SC 7	18 ^h 09 ^m 10.6 ^s	32 07 ^o 40 ⁰⁰	-0.14	-5.91	323	62335	2.12	0.94	0.90	0.99	1.29	2.25	4.35	
BUL_SC 8	18 ^h 23 ^m 06.2 ^s	21 47 ^o 53 ⁰⁰	10.48	-3.78	289	52542	2.10	0.88	0.83	0.91	1.15	1.94	3.74	
BUL_SC 9	18 ^h 24 ^m 02.5 ^s	21 47 ^o 55 ⁰⁰	10.59	-3.98	288	51264	1.82	0.89	0.84	0.88	1.14	1.92	3.67	
BUL_SC 10	18 ^h 20 ^m 06.6 ^s	22 23 ^o 03 ⁰⁰	9.64	-3.44	291	57049	1.88	0.97	0.91	0.94	1.22	2.09	4.05	
BUL_SC 11	18 ^h 21 ^m 06.5 ^s	22 23 ^o 05 ⁰⁰	9.74	-3.64	280	51168	1.84	1.00	0.90	0.92	1.19	1.96	3.78	
BUL_SC 12	18 ^h 16 ^m 06.3 ^s	23 57 ^o 54 ⁰⁰	7.80	-3.37	294	79146	2.29	0.99	0.90	0.98	1.32	2.34	4.67	
BUL_SC 13	18 ^h 17 ^m 02.6 ^s	23 57 ^o 44 ⁰⁰	7.91	-3.58	270	79044	2.25	1.04	1.00	1.04	1.44	2.47	4.89	
BUL_SC 14	17 ^h 47 ^m 02.7 ^s	23 07 ^o 30 ⁰⁰	5.23	2.81	290	90074	2.35	0.98	0.92	1.00	1.39	2.36	5.19	
BUL_SC 15	17 ^h 48 ^m 06.9 ^s	23 06 ^o 09 ⁰⁰	5.38	2.63	285	84337	2.27	0.96	0.92	1.00	1.36	2.22	4.84	
BUL_SC 16	18 ^h 10 ^m 05.7 ^s	26 18 ^o 05 ⁰⁰	5.10	-3.29	277	100861	2.34	1.01	0.92	1.01	1.40	2.55	5.48	
BUL_SC 17	18 ^h 11 ^m 03.6 ^s	26 12 ^o 35 ⁰⁰	5.28	-3.45	284	101916	2.27	0.95	0.91	1.01	1.39	2.57	5.47	
BUL_SC 18	18 ^h 07 ^m 03.5 ^s	27 12 ^o 48 ⁰⁰	3.97	-3.14	275	133236	2.53	0.97	0.90	1.06	1.45	2.90	6.62	
BUL_SC 19	18 ^h 08 ^m 02.4 ^s	27 12 ^o 45 ⁰⁰	4.08	-3.35	273	112389	2.38	0.96	0.89	0.99	1.34	2.50	5.81	
BUL_SC 20	17 ^h 59 ^m 19.1 ^s	28 52 ^o 55 ⁰⁰	1.68	-2.47	316	169339	2.81	1.01	0.98	1.14	1.66	3.35	8.08	
BUL_SC 21	18 ^h 00 ^m 22.3 ^s	28 51 ^o 45 ⁰⁰	1.80	-2.66	321	161147	2.77	1.01	0.97	1.13	1.62	3.33	7.75	
BUL_SC 22	17 ^h 56 ^m 47.6 ^s	30 47 ^o 46 ⁰⁰	-0.26	-2.95	414	111711	2.30	0.77	0.75	0.80	1.16	1.89	4.56	
BUL_SC 23	17 ^h 57 ^m 54.5 ^s	31 12 ^o 36 ⁰⁰	-0.50	-3.36	350	94777	2.13	0.78	0.71	0.76	1.07	1.71	4.08	
BUL_SC 24	17 ^h 53 ^m 17.9 ^s	32 52 ^o 45 ⁰⁰	-2.44	-3.36	359	91685	2.22	0.84	0.76	0.81	1.15	1.85	4.18	
BUL_SC 25	17 ^h 54 ^m 26.1 ^s	32 52 ^o 49 ⁰⁰	-2.32	-3.56	342	90821	2.41	0.82	0.75	0.82	1.10	1.82	4.27	
BUL_SC 26	17 ^h 47 ^m 15.5 ^s	34 59 ^o 31 ⁰⁰	-4.90	-3.37	346	95196	2.03	0.83	0.78	0.91	1.28	2.25	5.01	
BUL_SC 27	17 ^h 48 ^m 23.6 ^s	35 09 ^o 32 ⁰⁰	-4.92	-3.65	334	92482	2.15	0.85	0.80	0.91	1.25	2.19	4.87	
BUL_SC 28	17 ^h 47 ^m 05.8 ^s	37 07 ^o 47 ⁰⁰	-6.76	-4.42	321	57492	2.21	0.80	0.72	0.75	0.95	1.61	3.40	
BUL_SC 29	17 ^h 48 ^m 10.8 ^s	37 07 ^o 21 ⁰⁰	-6.64	-4.62	313	57810	2.36	0.76	0.70	0.74	0.94	1.62	3.38	
BUL_SC 30	18 ^h 01 ^m 25.0 ^s	28 49 ^o 55 ⁰⁰	1.94	-2.84	323	151819	2.76	0.91	0.87	1.03	1.49	2.93	7.04	
BUL_SC 31	18 ^h 02 ^m 22.6 ^s	28 37 ^o 21 ⁰⁰	2.23	-2.94	334	155341	2.24	0.94	0.90	1.08	1.51	3.09	7.40	
BUL_SC 32	18 ^h 03 ^m 26.8 ^s	28 38 ^o 02 ⁰⁰	2.34	-3.14	313	155014	2.40	0.94	0.91	1.09	1.54	3.21	7.54	
BUL_SC 33	18 ^h 05 ^m 30.9 ^s	28 52 ^o 50 ⁰⁰	2.35	-3.66	273	121800	2.62	0.92	0.84	0.99	1.32	2.54	5.99	
BUL_SC 34	17 ^h 58 ^m 18.5 ^s	29 07 ^o 50 ⁰⁰	1.35	-2.40	329	156179	2.56	0.99	0.94	1.14	1.68	3.03	7.52	
BUL_SC 35	18 ^h 04 ^m 28.6 ^s	27 56 ^o 56 ⁰⁰	3.05	-3.00	260	139289	2.56	0.96	0.89	1.03	1.43	2.85	6.77	
BUL_SC 36	18 ^h 05 ^m 31.2 ^s	27 56 ^o 44 ⁰⁰	3.16	-3.20	290	145288	2.74	1.01	0.95	1.10	1.53	3.25	7.90	
BUL_SC 37	17 ^h 52 ^m 32.2 ^s	29 57 ^o 44 ⁰⁰	0.00	-1.74	406	152630	2.47	0.72	0.69	0.83	1.23	2.11	4.46	
BUL_SC 38	18 ^h 01 ^m 28.0 ^s	29 57 ^o 01 ⁰⁰	0.97	-3.42	268	123366	2.43	0.92	0.88	1.02	1.40	2.64	6.40	
BUL_SC 39	17 ^h 55 ^m 39.1 ^s	29 44 ^o 52 ⁰⁰	0.53	-2.21	415	155642	2.82	0.77	0.74	0.88	1.35	2.24	5.50	
BUL_SC 40	17 ^h 51 ^m 06.1 ^s	33 15 ^o 11 ⁰⁰	-2.99	-3.14	325	82114	2.08	0.86	0.78	0.82	1.14	1.81	3.95	
BUL_SC 41	17 ^h 52 ^m 07.2 ^s	33 07 ^o 41 ⁰⁰	-2.78	-3.27	312	86985	2.45	0.87	0.82	0.86	1.20	1.92	4.30	
BUL_SC 42	18 ^h 09 ^m 05.0 ^s	26 51 ^o 53 ⁰⁰	4.48	-3.38	273	99107	2.39	0.95	0.91	0.99	1.41	2.47	5.28	
BUL_SC 43	17 ^h 35 ^m 13.5 ^s	27 11 ^o 00 ⁰⁰	0.37	2.95	382	76805	1.87	0.77	0.78	0.80	1.10	1.87	3.61	
BUL_SC 44	17 ^h 49 ^m 22.4 ^s	30 02 ^o 45 ⁰⁰	-0.43	-1.19	343	68440	1.90	0.84	0.84	0.88	1.14	1.95	3.73	
BUL_SC 45	18 ^h 03 ^m 36.5 ^s	30 05 ^o 00 ⁰⁰	0.98	-3.94	140	107345	3.24	1.67	1.63	1.83	2.42	4.61	10.56	
BUL_SC 46	18 ^h 04 ^m 39.7 ^s	30 05 ^o 11 ⁰⁰	1.09	-4.14	138	97186	3.32	1.79	1.68	1.81	2.35	4.38	10.38	
BUL_SC 47	17 ^h 27 ^m 03.7 ^s	39 47 ^o 16 ⁰⁰	-11.19	-2.60	242	47450	2.87	1.24	1.19	1.21	1.49	2.38	4.66	
BUL_SC 48	17 ^h 28 ^m 14.0 ^s	39 46 ^o 58 ⁰⁰	-11.07	-2.78	237	47674	2.51	1.29	1.21	1.18	1.46	2.37	4.63	
BUL_SC 49	17 ^h 29 ^m 25.1 ^s	40 16 ^o 21 ⁰⁰	-11.36	-3.25	234	43340	3.04	1.22	1.17	1.16	1.41	2.24	4.44	

In Fig. 1 we present with solid lines and open circles the best fit model of proper motion (μ ; σ) and positions allowing for the differential refraction respectively. As written in this figure, the parameters for this object are: eld SC 5-1-6, which means this object is in the OGLE-II eld BUL_SC 5, and sub eld (X,Y)=(1,6), OGLE ID=5930, $I = 14.304$, $V - I = 1.358$, the number of data points $N = 387$, proper motion (μ ; σ) = (1.30(0.36); 0.71(0.36)) (mas yr^{-1}) with a 1 errors in bracket. A Differential refraction coefficient is $a = 20.46$ mas.

We computed μ , σ , $\langle \mu \rangle$, and a for all stars used to transform coordinate systems (approximately the number of elds times the number of subframes times the typical number of stars per subframe, $49 \times 256 \times 400$). In cases when the star is measured in the overlap region of more than one subframe in a given eld, the data set with the largest number of points is selected. Stars with the number of data points fewer than 20 are rejected. The catalogue of whole BUL_SC 1 was recomputed in this analysis because

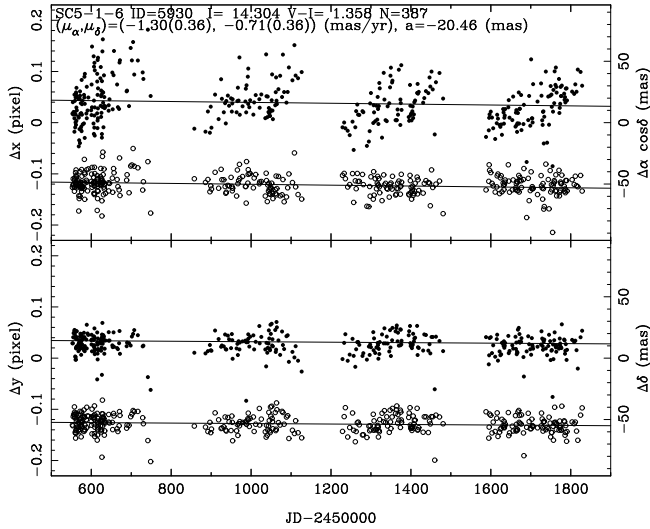


Figure 1. Time variation of the position in \cos (upper) and δ (lower) of star ID = 5930 ($V-I=1.358$) in BUL_SC 5. Filled circles represent actual positions, while open circles are positions corrected for differential refraction with a set of 0.16 pixels. Solid lines indicate a model fit of the proper motion $(\mu_\alpha; \mu_\delta) = (-1.30(0.36); -0.71(0.36))$ (mas yr^{-1}) with a 1 σ errors in bracket. A differential refraction coefficient is $a = -20.46$ mas.

the catalogue presented by Sumi, Eyer & Wozniak (2003) contain only 70 % of this field.

Our catalog contain 5,078,188 stars, which is 79.8 % of all objects with $I < 18$ mag in the original OGLE template (Udalski et al. 2002). 7% of these stars don't have any V -band photometry. The missing V -band photometry of stars might be known according to the differential refraction coefficient because there is good correlation between the differential refraction coefficient a and the apparent $V-I$ colour for stars (see Fig. 3), if they are same population as that of the majority.

4 HIGH PROPER MOTION OBJECTS

The detectability of high proper motion is limited by the search radius used for cross-identification of stars on all images. The search radius, 1 pixel yr^{-1} , corresponds to 400 mas yr^{-1} . Objects with 100 mas yr^{-1} cannot be identified over the full four year long observing interval of OGLE-II, as they move out of the search radius. In order to be able to follow fast moving stars over four observing seasons we made additional astrometry for objects for which preliminary estimate gave proper motion $> 100 \text{ mas yr}^{-1}$. Whenever a star moved more than 0.4 pixels from the previous search center we moved that center to the median location of the last 3 data points. This procedure was adopted when it allowed us to locate the star in a larger number of CCD images. It was applied to 262 objects out of the total of 640 which have $> 100 \text{ mas yr}^{-1}$.

We show the positional movement of one of the highest proper motion objects in Fig. 2. This star have relatively fewer data points because this is overexposed on the good seeing frames in the I band. The photometry is highly

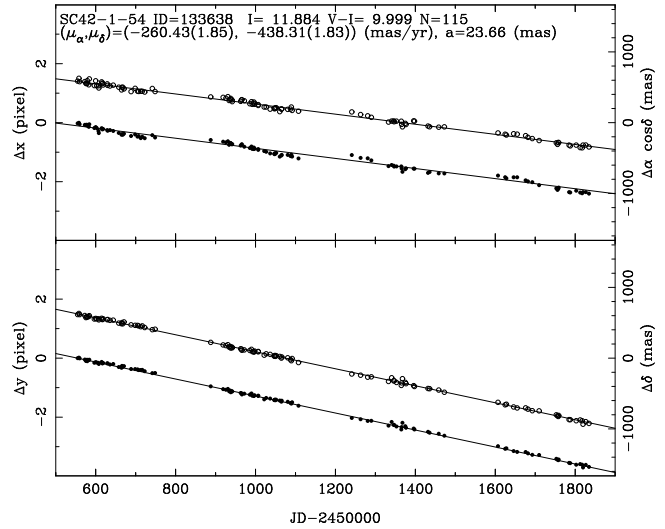


Figure 2. Same plots as Fig. 1 for ID = 133638 ($V-I$ =none) in OGLE-II field BUL_SC 42, one of the highest proper motion star. Filled circles represent actual positions and open circles are the positions corrected for differential refraction, with a set of +1.5 pixels. Solid lines indicate a model fit of the proper motion $(\mu_\alpha; \mu_\delta) = (-260.43(1.85); -438.31(1.83))$ (mas yr^{-1}) with a 1 σ errors in bracket. A differential refraction coefficient is $a = 23.66$ mas, which indicates the star is very red. The photometry is highly unreliable and doesn't have V -band magnitude because if the star has a significant proper motion. The photometry of the star obtained by hand relatively to the neighboring stars is: $I = 11.70$, $V-I = 2.86$.

unreliable because if the star has a significant proper motion - it cannot be measured precisely in the "fixed position mode" over years. The star does not have V -band measurements because it considerably moved during the time between the I-band and V -band template images were taken. Therefore cross-identification failed. The photometry of the star obtained by hand relatively to the neighboring stars is: $I = 11.70$, $V-I = 2.86$. This color is very red as expected from the relation between differential refraction coefficient a from the I and color in Fig. 3, but its a and $V-I$ does not match the relation exactly.

The relation of a and $V-I$ for BUL_SC 42 in which the extinctions are relatively small, is similar with but somewhat different from that for BUL_SC 5 plotted in Fig. 3. The zero-point of a is 15 mas higher than that for BUL_SC 5. But expected colour of this star from this relation is still redder ($V-I = 4.5$). In these figures the slopes of them are different in $V-I > 3$. This is because of the difference of the population. In BUL_SC 5 majority in this colour region are RCGs and Red Giant Branch stars, but Red Super Giants in BUL_SC 42. So this disagreement might be because this object is nearby very red dwarf of $M 4-5$ spectral type, not the majority of this catalog.

5 CATALOGUE

A sample of our catalog of proper motions is shown in Table 2. The complete list of all 5,078,188 stars is available in electronic form at via anonymous ftp from the server

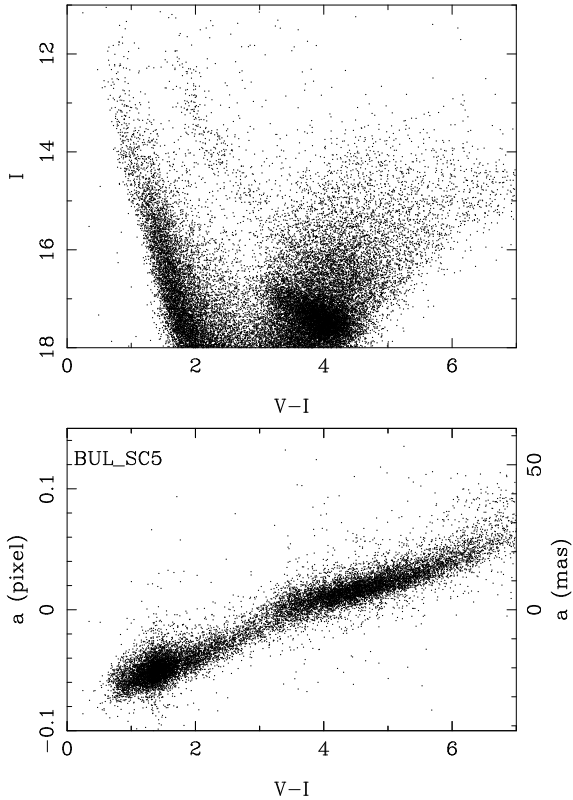


Figure 3. Upper: Colour-magnitude diagram of the half of the analyzed stars in OGLE-II field BUL_SC5. Lower: correlation between the differential refraction coefficient a and the apparent colour for stars with $I < 16$ in this field.

ftp://ftp.astrouw.edu.pl/ogle/ogle2/proper_motion/ and ftp://bulge.princeton.edu/ogle/ogle2/proper_motion/. The list contains star ID, number of data points N , measured and with their errors, a , standard deviation (Sdev) of data points in the fitting, equatorial coordinates, apparent I-band magnitude and $V-I$ colour. ID, 2000 coordinates, I and $V-I$ for each object are identical with those in Udalski et al. (2002). If the object doesn't have V-band photometry the $V-I$ colour is written as 9.999.

Note, the number of data points N differs from star to star even if they have similar brightness. This is because some are near the edge of the CCD in age or CCD defects, and others are affected by blending. We use the positions which is categorized as a single isolated star by DOPHOT. Hence, blended stars can not be measured when the seeing is poor.

In Fig. 3 we present a colour-magnitude diagram (CMD) for stars in OGLE field BUL_SC5, which is one of the most reddened OGLE-II fields. We also show the correlation between the differential refraction coefficient a and the apparent $V-I$ colour for stars with $I < 16$ in this field. This correlation for other fields are similar but slightly different depending on the population of the majority in each field. In Fig. 4, we plot the uncertainty in $\mu = \sqrt{\sigma_{\cos}^2 + \sigma_{\mu}^2}$, in BUL_SC5 as a function of the apparent I-band magnitude. Also plotted is the mean uncertainty $\langle \mu \rangle$ with 2 clipping as a function of I (open circle); these are also listed in Table 1. Note: that the accuracy of proper motions in our catalogue is better than 1 mas yr^{-1} for $12 < I < 14$.

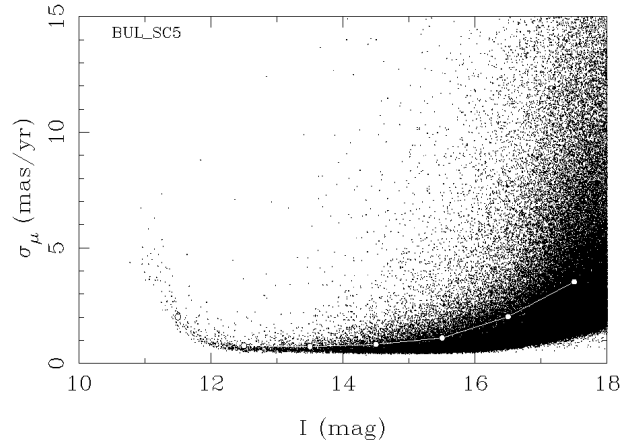


Figure 4. Uncertainty in μ in OGLE-II field BUL_SC5 as a function of the I-band magnitude I . Open circles are mean values for each 1 magnitude bin.

To check our measurements we cross-identified stars in our catalog with the Tycho-2 catalog (Høg et al. 2000). We selected from our catalog objects with the proper motion higher than 10 mas yr^{-1} , and measured with a significance above 3, to avoid mis-identification. Most of high proper motion stars in Tycho-2 are saturated in OGLE in ages. We found 58 Tycho-2 stars in our catalog and their proper motions: $\mu_{\text{Tycho-2}}$ (thin) and μ_{OGLE} (thick) are presented in Fig. 5. We can see a very good correlation between our and Tycho-2 measurements. Dashed lines indicate $\mu_{\text{OGLE}} = \mu_{\text{Tycho-2}}$, and solid lines represent best fit with the fixed unit slope and a possible offset. The measured offsets: $\mu_{\text{Tycho-2}} - \mu_{\text{OGLE}} = 3:39 \text{ mas yr}^{-1}$ and $\mu_{\text{Tycho-2}} - \mu_{\text{OGLE}} = 6:63 \text{ mas yr}^{-1}$ are roughly consistent with what is expected if our proper motions are measured with respect to the frame defined by the average proper motion of stars located in the Galactic Bulge, which is presumably close to absolute proper motion of the Galactic Center (GC). The latter is estimated to be $(\mu_{GC}; \nu_{GC}) = (2:9; 5:0) \text{ mas yr}^{-1}$ assuming a rotation curve of $v_r = 220 \text{ km s}^{-1}$ and Solar velocity of 19 km s^{-1} toward $(l; b) = (53; 25)$ relative to the Local Standard of Rest (LSR) (Binney & Tremaine 1987), i.e., $(v_l; v_b) = (12 \text{ km s}^{-1}, 7 \text{ km s}^{-1})$. A good correspondence between the Tycho-2 - OGLE-II offset and the expected proper motion of the Galactic Center gives us certain confidence in our measurements.

We also compared the measurements in BUL_SC1 made by Sumi, Eyer & Wozniak 2003 (hereafter SC1⁰) with the proper motion presented in this paper, for which our measurements are above 10 level of accuracy. The two sets of proper motions for 1367 cross-identified stars are shown in Fig. 6 together with the best fit line. The offset between the two sets, and the differences between individual measurements are within estimated errors. Note: the scale is different than in Fig. 5.

We compared the measurements done by us in one of the overlap regions: between fields BUL_SC1 and BUL_SC45. The proper motions of 133 cross-identified stars, and the best fit with a small offset between the zero points are presented in Fig. 7. A rather large zero point offset is:

$$\mu_{\text{SC1}} - \mu_{\text{SC45}} = 2:64 \text{ mas yr}^{-1} \text{ and } \nu_{\text{SC1}} - \nu_{\text{SC45}} =$$

Table 2. Sample of fitted parameters in the catalog for BIL_SC2.

ID	N	cos	\cos (m asyr ⁻¹)			a	Sdev	2000	2000	I	V	I
						(m as)		(deg)	(deg.)		(m ag)	
79060	259	4.66	0.48	-3.12	0.48	-9.71	9.03	271.0029165	-28.9917500	14.233	0.842	
79061	263	0.07	0.36	0.15	0.36	1.10	6.89	271.0084590	-28.9918333	14.850	1.650	
79062	258	-0.34	1.01	-5.73	1.01	7.36	18.89	271.0418745	-28.9909167	14.666	1.578	
79063	164	23.95	2.80	14.72	2.80	-1.32	43.13	270.9888330	-28.9905278	14.610	1.784	
79064	119	1.40	0.83	-2.25	0.82	2.10	11.29	270.9859995	-28.9900000	14.465	2.300	
79065	252	1.54	0.76	-1.68	0.76	1.05	14.12	271.0111245	-28.9901389	14.792	1.452	
79066	103	-3.02	1.31	-1.60	1.31	-7.92	15.89	271.0331670	-28.9900833	13.980	1.813	
79067	264	1.95	0.62	1.32	0.62	-4.16	11.76	271.0178340	-28.9893889	14.268	0.826	
79068	248	3.35	0.51	-1.59	0.51	0.51	9.41	270.9994590	-28.9891111	14.201	1.596	
79069	264	-4.38	0.51	-2.88	0.51	4.14	9.66	271.0242495	-28.9889167	14.599	2.096	
79071	264	0.78	0.48	2.20	0.48	-0.82	9.19	271.0473750	-28.9885000	14.044	2.021	
79072	261	-4.34	0.46	-6.63	0.46	4.15	8.63	271.0173750	-28.9884444	14.668	1.754	
79073	264	-3.70	0.45	0.97	0.45	0.20	8.45	271.0253745	-28.9878889	14.207	1.690	
79074	264	3.82	0.56	3.55	0.56	-2.21	10.57	271.0305000	-28.9879167	14.631	1.395	
79075	264	-0.66	0.41	-2.59	0.41	-0.07	7.75	271.0112085	-28.9866944	14.038	1.548	
79076	264	5.42	0.52	3.76	0.51	-1.73	9.75	271.0425000	-28.9865556	14.403	1.623	
79077	264	6.18	0.41	-1.49	0.41	5.34	7.87	271.0467495	-28.9858889	14.164	2.257	
79078	264	0.68	0.74	1.90	0.73	2.15	13.93	271.0267500	-28.9852222	14.742	1.896	
79079	262	2.29	0.75	1.66	0.75	0.06	14.16	271.0389585	-28.9848056	14.441	1.950	
79080	263	-0.04	0.52	-0.06	0.52	5.94	9.81	271.0097505	-28.9843889	14.774	2.105	
79082	133	4.47	0.80	0.55	0.79	9.26	10.43	271.0467495	-28.9841111	14.265	2.187	

0.25 m asyr⁻¹, while the scatter is consistent with the estimated errors. The offset indicates the scale of possible systematic errors in our measurements, which are done with respect to the average motion of all stars within an analyzed sub-frame. We shall discuss this issue in section 7.

Fig. 8 shows the histogram of our proper motion measurements for the whole catalog, with the lines with increasing thickness corresponding to all stars, and to those detected with confidence better than 3, 5 and 10, respectively. The total number of stars with the proper motion measured with 3, 5 and 10 accuracy is $N_3 = 1;534;379$, $N_5 = 626;365$, $N_{10} = 78;757$, respectively. The inclined solid line: $\log(N) = 3\log(\mu) + \text{const}$, has a slope corresponding to the expectation for a uniform distribution and kinematics of stars in space. The distribution of accurate (5 and 10) proper motions seems to be roughly consistent with the uniform distribution.

However, the number of very high proper motion stars, ($\mu > 200$ m asyr⁻¹), appears to be smaller than expected from a uniform distribution. This may be due to saturation of in ages of nearby, and therefore apparently bright, stars in OGLE in ages.

The distribution of less accurate ($\mu < 3$) proper motions have an apparent cut-off at 100 m asyr⁻¹. Such stars are apparently faint, their positions have large errors, and they may be difficult to identify in a search radius of 1 pixel, which corresponds to 100 m asyr⁻¹.

A more thorough analysis of various selection effects is beyond the scope of this paper. Readers are advised to use caution in a statistical analysis of our catalog.

6 POSSIBLE PROBLEMS

There may be various problems with proper motion of variable stars. Our fields are very crowded, hence many stars

may be blended. In case of blending we measure some average position of a blend of several stars within a seeing disk. If a variable star is blended with other stars which have slightly different position within a seeing disk, the average of position of the blended image may change while one component of the blend varies. This change might mimic a proper motion.

As an example we present time variation of the position of a very long timescale microlensing event candidate (Smith (2003)) in top panel of Fig. 9. The I-band light curve of this event is shown in the bottom panel of Fig. 9 (ID = 2859 in variable star catalog of Wozniak et al. 2001). In the top panel we can see an apparent proper motion in first year which is coincident with the apparent brightness fading, as shown in the bottom panel. After the second year the proper motion seems to be small, and the position data points are sparse, which coincides with low brightness of the star and may reflect the presence of a blend (in poor seeing DOPHOT cannot resolve the two stars, hence very few data points in the upper panel. The blend was actually found in the higher resolution OGLE-III in ages in 2002.

A plausible interpretation is that the microlensed star was brighter than the nearby faint 'companion' star in 1997, but by 2000 it became fainter of the two. The position of the 'companion' is consistent with the direction of the apparent proper motion. The faint stars seem to have low proper motion. High resolution observations are needed to fully understand this object.

As another example we present in Fig. 10 time variation of the position of a star ID = 309705 in the OGLE-II field BUL_SC 39. Filled circles represent measured positions with type=1 (used in this work) which was at a fixed location for the first three years, and moved significantly in the fourth season. The star ID = 309705 identified these centroids at edge of search radius ($y = -1$) for first 3 seasons and at the center ($y = 0$) in the 4th season. On the other hand,

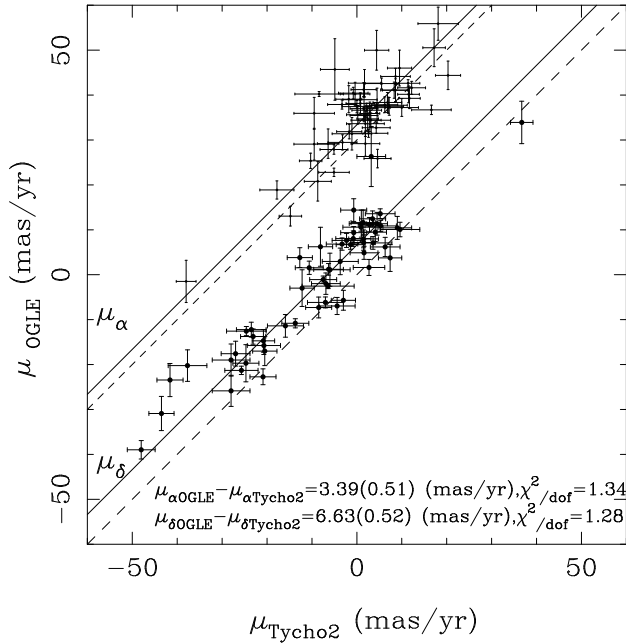


Figure 5. Comparison of proper motions (thin and thick) for 58 stars cross-identified in our catalog and in Tycho-2 catalog. Dashed lines indicate $\mu_{OGLE} = \mu_{Tycho2}$, and solid lines represent the best fit with the datasets: $\mu_{\alpha,OGLE} = 3.39$ $m\ asy\ r^{-1}$ and $\mu_{\delta,Tycho2} = 6.63$ $m\ asy\ r^{-1}$. These are roughly consistent with the expectation if our frame of references corresponds to the stars located in the Galactic Bulge and moving (on average) with the Galactic Center with respect to the inertial frame of Tycho-2. μ_{α} and μ_{δ} are shifted for +30 $m\ asy\ r^{-1}$ for clarity.

neighboring star ID = 309653 which have similar brightness of $I = 14.8$ and position of 0.18 pixels East (positive x) and -1.89 pixels South (negative y), identified same centroids at the edge of search radius ($y = +1$).

To see the detail of this object, in Fig. 10 we also plot the position measurements which is categorized as a star blended with other star (type=3, which are not used in this work) by DoPHOT for this star (crosses) and neighboring star ID = 309653 (dots), which are shifted by +0.18 pixels in x and -1.89 pixels in y, i.e. these dots are as they are on CCD, relative to ID = 309705. We can see that these positions (crosses and dots) are around the center of them $y = 0$ (ID = 309705) and -2 (ID = 309653) respectively and filled circles are in-between of them. We also show the light curves I-band of ID = 309705 (middle panel) and ID = 309653 (bottom panel) in Fig. 10. We can see ID = 309705 is constant during four seasons but ID = 309653 suddenly faded at 4th season. This is likely to be a RCMB type variable.

The simplest interpretation is as follows; Small number of data points in the seasons 1997-99 indicates that DoPHOT found that object which is composite of these two stars only on the bad seeing frames as a single star with type=1, in other cases they are separated but categorized as blended-type=3. In 2000 when the star ID = 309653 faded, the centroid of the composite moved and finally the star ID = 309705 became "single" star with type=1. So the number of data points is large in 2000.

Proper motions of variable stars may have their errors increased not only because of variable contribution of blend-

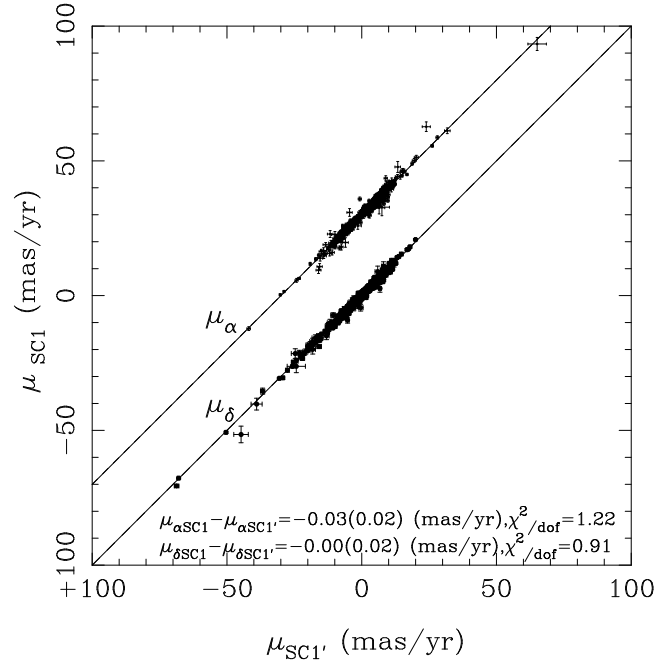


Figure 6. Same figure as Fig. 5 for 1367 stars cross-identified in BUL_SC1 by Sumi, Eyer & Wozniak 2003 (hereafter SC1⁰) and in SC1 by this work, measured with better than 10 level accuracy. Dashed lines indicate $\mu_{SC1} = \mu_{SC1^0}$ which overlap with the solid line in this case, and solid lines represent the best fit with the datasets: $\mu_{\alpha,SC1} = -0.03$ $m\ asy\ r^{-1}$ and $\mu_{\delta,SC1^0} = 0.00$ $m\ asy\ r^{-1}$. μ_{α} and μ_{δ} are shifted for +30 $m\ asy\ r^{-1}$ for clarity. Note: the scale is different from Fig. 5.

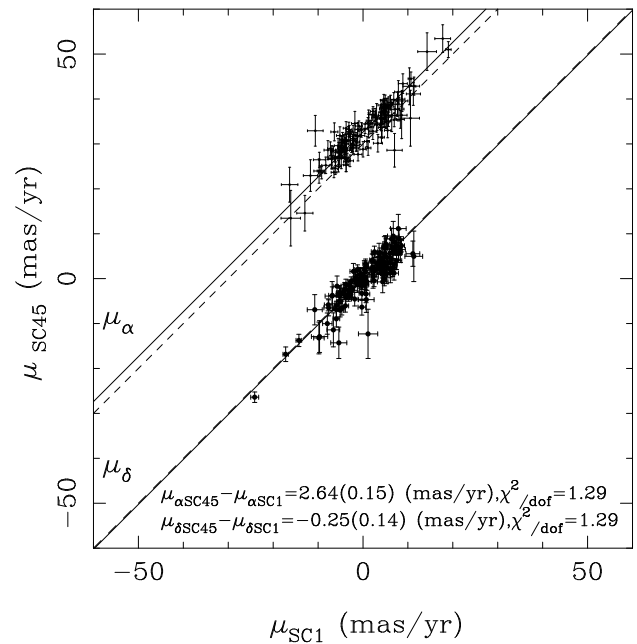


Figure 7. Same figure as Fig. 5 for 133 stars cross-identified in the overlap region between OGLE-II fields BUL_SC1 and BUL_SC45, and measured with better than 5 level accuracy. Dashed lines indicate $\mu_{SC1} = \mu_{SC45}$, and solid lines represent the best fit with the datasets: $\mu_{\alpha,SC1} = 2.64$ $m\ asy\ r^{-1}$ and $\mu_{\delta,SC45} = -0.25$ $m\ asy\ r^{-1}$ in SC45 are shifted for +30 $m\ asy\ r^{-1}$ for clarity.

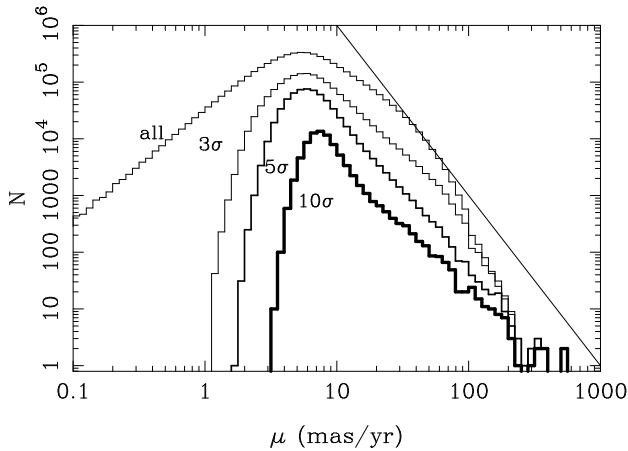


Figure 8. Histograms are shown for all $N = 5,078,188$ stars, and for measurements with confidence better than 3 , 5 and 10 (from the thinnest to the thickest line, respectively) for all 49 OGLE-II fields. The total number of stars with proper motion with 3 , 5 and 10 accuracy are $N_3 = 1534379$, $N_5 = 626365$, $N_{10} = 78757$. The inclined solid line: $\log(N) = 3\log(\mu) + \text{const}$: has the slope expected if the stars have a uniform distribution and kinematics.

ing, but also because variable stars may change colors, and therefore the coefficient of differential refraction may also change. In rare cases of very long period variables this may be noticeable. Note: we do not treat this kind of objects in a special way, so a reader must be careful while using our catalog in studies of variable stars.

The effect of blending changes with seeing may contribute to the scatter of data points, but it is not likely to have a seasonal effect. Hence, we think that seeing variation are not a major problem.

The probability of blending is much larger for fainter stars, in particular those close to $I = 18$ mag. This may produce a bias in their proper motions, most likely reducing their formal proper motion, as the blended stars may have a different proper motion vector, so the average value is likely to be reduced. We also do not provide a special treatment for this kind of objects, so a reader must be careful while using our catalog for faint stars.

7 DISCUSSION AND CONCLUSION

We have measured proper motions for 5,078,188 stars in all 49 OGLE-II Galactic Bulge fields, covering a range of $11 < l < 11$ and $6 < b < 3$. Our catalogue contains objects with proper motion of up to ≈ 500 mas yr $^{-1}$ and I-band magnitude in the range $11 < I < 18$. The accuracy of proper motions in our catalogue is better than 1 mas yr $^{-1}$ for $12 < I < 14$.

One should keep in mind that all measurements of $\langle \mu \rangle$ presented here are not absolute, but relative to the astrometric reference frame which is roughly that of the Galactic Center. However, as demonstrated with a comparison of measurements in the overlap region of fields BUL_SC1 and BUL_SC45 (cf. Fig. 7), the frame of references is not very stable. This problem will be partly solved by using background quasars which may be detected in the near future

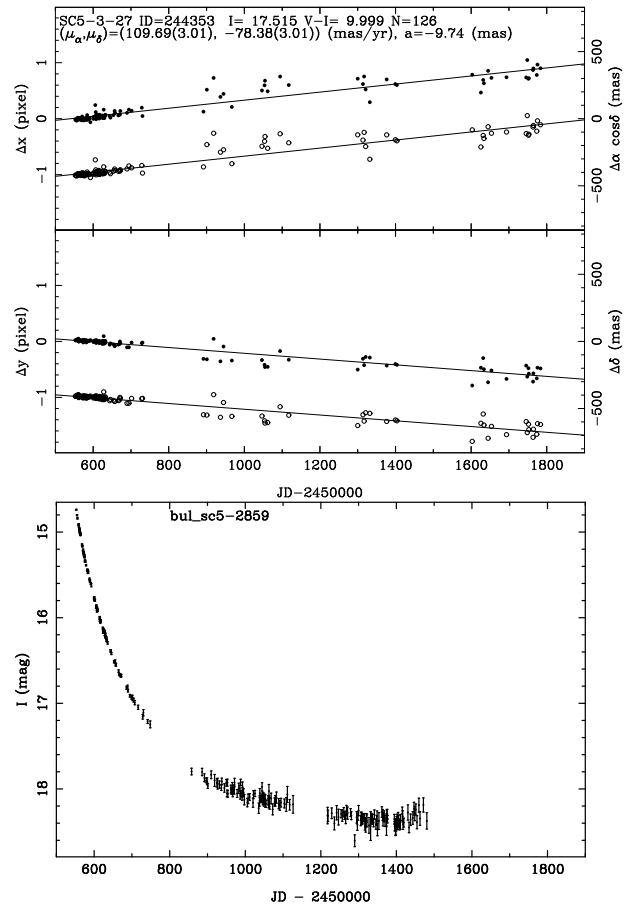


Figure 9. Top panel: Same plots as Fig. 1 for the star ID = 244353 in the OGLE-II field BUL_SC5. Filled circles represent actual positions and open circles correspond to positions corrected for differential refraction, with the offset of 1 pixels. Bottom panel: I-band light curve of same star (ID = 2859 in catalog of Wozniak et al. 2001), a possible very long microlensing event.

using the OGLE-II variability catalog (Wozniak et al. 2002; Eyer 2002; Dobrzycki 2003).

As demonstrated by Sumi, Eyer & Wozniak (2003), the proper motions based on OGLE-II data can be used to clearly detect the presence of a strong streaming motion (rotation) of stars in the Galactic bar. While the reference frame established by the large number of stars is not well defined with respect to the inertial frame of reference, the relative motions of groups of stars within a given field are well determined.

Though our primary goal is to constrain the Galactic bar model with the future analysis of our catalog, we provide proper motions for all stars with $I < 18$ mag in all 49 OGLE-II Galactic bulge fields because this catalog might be useful for variety of projects. An analysis of the catalog is beyond the scope of the present study.

In the near future we shall present extinction maps in all 49 OGLE-II Galactic bulge fields, which will facilitate study of the Galactic structure. A thorough analysis of all available data is underway and will be published elsewhere.

ACKNOWLEDGMENTS

We are grateful to B. Paczynski for helpful comments and discussions. T.S. acknowledge the financial support from the Nishina Memorial Foundation and JSPS. The paper was partly supported by the Polish KBN grant 2P 03D 02124 to A. Udalski. This work was partly supported with the following grants to B. Paczynski: NSF grants AST-9820314 and AST-0204908, and NASA grants NAG 5-12212, and grant HST-AR-09518.01A provided by NASA through a grant from the Space Telescope Science Institute, which is operated by the Association of Universities for Research in Astronomy, Inc., under NASA contract NAS5-26555.

REFERENCES

- Afonso, C. et al. 2003, *A&A* in press, preprint (astro-ph/0303100)
- Alcock, C. et al. 1997, *ApJ*, 486, 697
- Alcock, C. et al. 2000a, *ApJ*, 541, 734
- Aubourg, E. et al. 1993, *Nature*, 365, 623
- Binney, J. & Tremaine, S. 1987, *Galactic Dynamics* (Princeton: NJ, Princeton University Press)
- Blitz, L. & Spergel, D.N.S. 1991, *ApJ*, 379, 631
- Bond, I.A. et al. 2001, *MNRAS*, 327, 868
- de Vaucouleurs, G. 1964. *IAU Symp. 20. The Galaxy and the Magellanic Clouds*, ed. F. J. Kerr & A. W. Rogers (Canberra: Australian Acad. Science, M SSSO), 195
- Dobrzycki, A. et al. 2003, *AJ*, 125, 1330
- Eyer, L. & Wozniak, P.R. 2001, *MNRAS*, 327, 601
- Eyer, L. 2002, *Acta Astronomica*, 52, 241
- Gould, A. 1996, *PASP*, 108, 465
- Hafner, R. et al. 2000, *MNRAS*, 314, 433
- Høg et al. 2000, *A&A*, 355, L27
- Kiraga, M., & Paczynski, B. 1994, *ApJ*, 430, L101
- Kuijken, K. & Rich, R.M. 2002, *AJ*, 124, 2054
- Mao, S. & Paczynski, B. 2002, preprint (astro-ph/0207131)
- Monet, D. et al. 2002, preprint (astro-ph/0210694)
- Paczynski, B. 1996, *ARA&A*, 34, 419
- Paczynski, B. & Stanek, K.Z. 1998, *ApJ*, 494, L219
- Popowski, P. 2003, *Invited Review*, to appear in "Gravitational Lensing: A Unique Tool For Cosmology", *Aussois 2003*, eds. D. Valls-Gabaud & J.-P. Kneib (astro-ph/0304464)
- Salin, S. & Gould, A. 2003, *ApJ*, 582, 1011
- Schechter, L., Mateo, M., & Saha, A. 1993, *PASP*, 105, 1342S
- Smith, M.C., 2003, *MNRAS* in press (astro-ph/0304442)
- Spaenhauer, A., Jones, B.F. & Whitford, A.E. 1992, *AJ*, 103, 297
- Stanek, K.Z. 1996, *ApJ*, 460, 37L
- Stanek, K.Z. et al. 1994, *ApJ*, 429, L73
- Stanek, K.Z. et al. 1997, *ApJ*, 477, 163
- Stanek, K.Z. et al. 2000, *Acta Astronomica*, 50, 191
- Sumi, T., Eyer, L. & Wozniak, P.R. 2003, *MNRAS*, 340, 1346
- Sumi, T. et al. 2002, *ApJ* in press, preprint (astro-ph/0207604)
- Udalski, A. et al. 1993, *Acta Astron.*, 43, 289
- Udalski, A. et al. 1994, *Acta Astronomica*, 44, 165
- Udalski, A. et al. 2000, *Acta Astronomica*, 50, 1
- Udalski, A. et al. 2002, *Acta Astronomica*, 52, 217
- Udalski, A., Kubiak, M., & Szymanski, M. 1997, *Acta Astronomica*, 74, 319
- Wozniak, P.R., et al. 2001, *Acta Astronomica*, 51, 175
- Wozniak, P.R., et al. 2002, *Acta Astronomica*, 52, 129

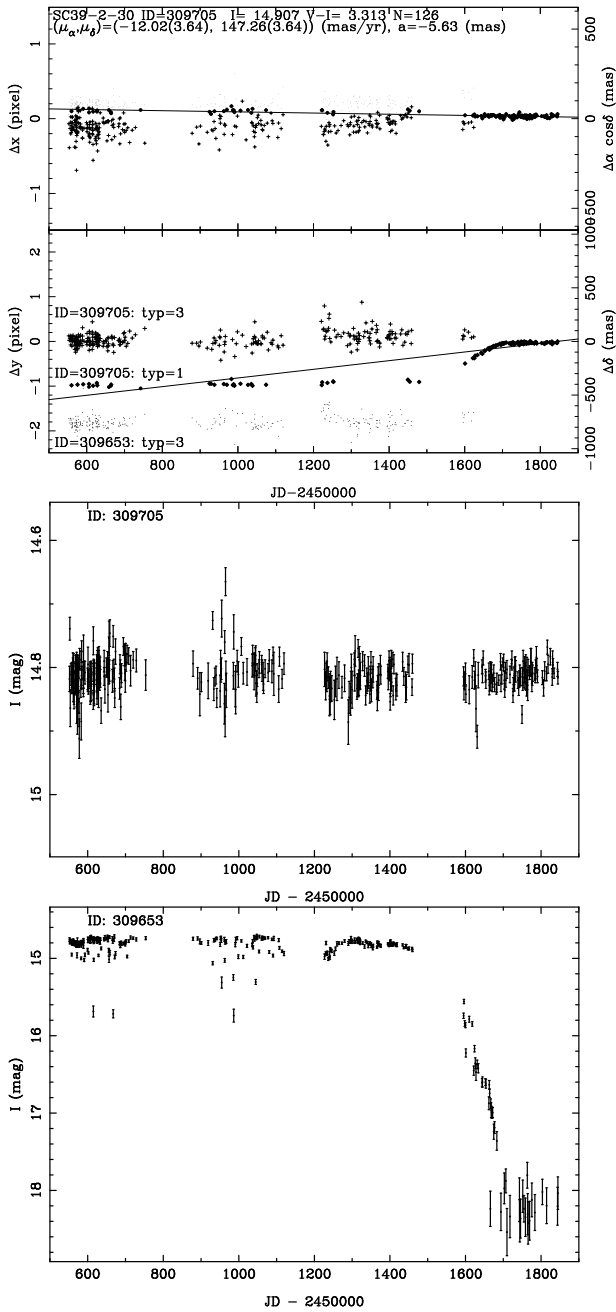


Figure 10. Top: Same plots as Fig. 1 for star ID = 309705 in OGLE-II field BUL_SC 39. Filled circles represent actual positions with type= 1 (used in this work), crosses correspond to position measurements with type= 3 (not used) and dots indicate positions measurements of neighboring star ID = 309653 with type= 3 which are shifted by +0.18 pixels in x and -1.89 pixels in y, i.e. these dots are as they are on CCD, relative to ID = 309705. This is a probable case of a blend with one component being a variable star.